REFINED POINTWISE ESTIMATES FOR A 1D VISCOUS COMPRESSIBLE FLOW AND THE LONG-TIME BEHAVIOR OF A POINT MASS

KAI KOIKE

ABSTRACT. We present results on the long-time behavior of a point mass moving in a 1D viscous compressible fluid. In a previous work, we showed that the velocity $V(t)$ of the point mass decays at least as $t^{-3/2}$. In this note, we give a necessary and sufficient condition on the initial data for the decay rate $3/2$ to be optimal. This result is obtained as a corollary to refined pointwise estimates for solutions to the barotropic compressible Navier–Stokes equations. This note is a résumé of the preprint [3] with some numerical results added. Our intention is to explain, in a concise manner, the core idea behind the somewhat lengthy calculations given there.

CONTENTS

1. INTRODUCTION

Phenomena arising from interaction of moving solids with fluid flows are studied intensively by many mathematicians. One of the reasons why such problems attract mathematicians is because coupling of equations of motion for fluid and solid creates new phenomena and impetuses for development of new theories.

In this note, we consider the motion of a point mass in a viscous compressible fluid. In a previous work [4], we showed that the velocity $V(t)$ of the point mass decays at least as $t^{-3/2}$. Here, we give a simple necessary and sufficient condition on the initial data for the optimality of the decay rate $3/2$.

In the rest of this section, we explain the formulation of the problem. Then, in Section 2, we state the main theorem and discuss its consequences. The idea of the proof is explained in Section 3. Here, we tried to reveal the scaffolding of the proof rather than to explain the proof in detail; for the detail, we refer to [3]. Finally, we report in Section 4 some numerical simulations related to the main theorem.

1.1. Point mass motion in a viscous compressible fluid: Formulation.

Let us imagine an infinitely long channel in which a fluid is filled; the channel is then separated into two chambers by a movable piston (see Figure 1). Although the figure is multi-dimensional, we stress here that we consider a one-dimensional problem: we assume that the fluid variables, i.e., the density ρ and the velocity field U only depend on the spatial coordinate X whose axis is parallel to the channel walls (the hatched

regions in Figure 1) and the time variable t. We also neglect the thickness of the piston. Hence, if we project the system onto the X-axis, we can regard the piston as a point mass moving in a one-dimensional flow. This justifies the title of this note. The word used depends on the authors: For example, in [9], the solid is called a piston, and in [10], it is called a point mass (or a point particle).

We assume that the fluid is viscous, compressible, and barotropic. Here, *barotropic* means that the pressure P of the fluid is a function only of the density ρ, that is, $P = P(\rho)$. The barotropic assumption is valid, for example, if either the temperature or the entropy remains almost constant (*isothermal* or *isentropic* flows). This assumption is usually not so realistic but is assumed here for simplicity. As for the point mass, we assume that its motion is governed by Newton's second law.

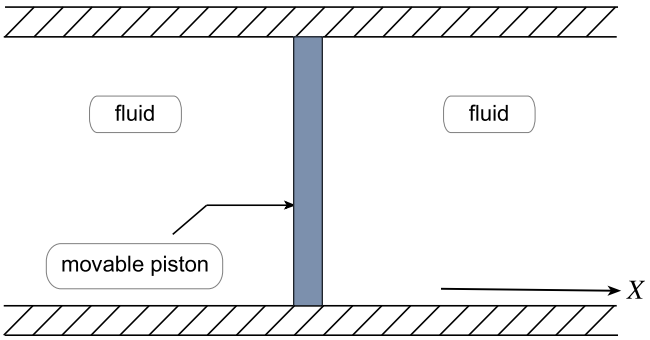

FIGURE 1. A movable piston separates an infinite channel into two semi-infinite chambers in which two fluids of the same kind flow.

With these assumptions, we can write down the equations describing the motion of the fluid and the point mass:

$$
(1)\qquad \begin{cases} \rho_t + (\rho U)_X = 0, & X \in \mathbb{R}\backslash\{h(t)\},\ t > 0, \\ (\rho U)_t + \left(\rho U^2\right)_X + P(\rho)_X = \nu U_{XX}, & X \in \mathbb{R}\backslash\{h(t)\},\ t > 0, \\ U(h(t)^+, t) = U(h(t)^-, t) = V(t), & t > 0, \\ mV'(t) = [\![-P(\rho) + \nu U_X]\!](h(t), t), & t > 0, \\ h(0) = h_0,\ V(0) = V_0;\ \rho(X,0) = \rho_0(X),\ U(X,0) = U_0(X), & X \in \mathbb{R}\backslash\{h_0\}. \end{cases}
$$

Here, $\rho = \rho(X,t)$ and $U = U(X,t)$ are the density and the velocity of the fluid, and $\nu > 0$ and $P = P(\rho)$ are the viscosity and the pressure; $h = h(t)$ and $V = V(t) = h'(t)$ are the position and the velocity of the point mass, and m is its mass. Hereafter, we set $m = 1$ for simplicity. The double brackets $[\![f]\!](X,t)$ are defined by $[\![f]\!](X,t) := f(X^+,t) - f(X^-,t)$, where $f(X^\pm,t) = \lim_{Y \to X^\pm} f(Y,t)$.[1] The first two equations are the one-dimensional barotropic compressible Navier–Stokes equations; the third equations are the boundary conditions for the Navier–Stokes equations, which say that the fluid does not penetrate through the point mass. The fourth equation is Newton's second law; the right-hand side is the net fluid force on the point mass. The final set of equations are the initial conditions.

The equations above are posed in a time-dependent domain $\mathbb{R}\backslash\{h(t)\}$. For ease of mathematical analysis, we transform the domain into a time-independent one. To do so, we introduce *the Lagrangian*

[1] $\lim_{Y \to X^+}$ and $\lim_{Y \to X^-}$ denote the limit from the right and the left, respectively.

mass coordinate. Fix $x \in \mathbb{R}_* := \mathbb{R}\backslash\{0\}$ and $t \geq 0$, and let $X = X(x,t)$ be the solution to

$$x = \int_{h(t)}^{X(x,t)} \rho(X',t)\, dX'.$$

Here, ρ is the solution to (1). We assume that $\rho(x,t) \geq \rho_0$ for some $\rho_0 > 0$. Then the equation above is uniquely solvable and determines a one-to-one map

$$\mathbb{R}_* \ni x \mapsto X(x,t) \in \mathbb{R}\backslash\{h(t)\}.$$

The Lagrangian mass coordinate is this variable x. We also change the dependent variables as follows:

$$v(x,t) = \frac{1}{\rho(X(x,t),t)}, \quad u(x,t) = U(X(x,t),t), \quad p(v) = P\left(\frac{1}{v}\right).$$

Using the first equation in (1), we can show that

$$\frac{\partial X(x,t)}{\partial x} = v, \quad \frac{\partial X(x,t)}{\partial t} = u. \tag{2}$$

With these in mind, we can check that (1) is equivalent to

$$\begin{cases} v_t - u_x = 0, & x \in \mathbb{R}_*,\ t > 0, \\ u_t + p(v)_x = \nu \left(\dfrac{u_x}{v}\right)_x, & x \in \mathbb{R}_*,\ t > 0, \\ u(0^+,t) = u(0^-,t) = V(t), & t > 0, \\ V'(t) = [\![-p(v) + \nu u_x/v]\!](t), & t > 0, \\ V(0) = V_0;\ v(x,0) = v_0(x),\ u(x,0) = u_0(x), & x \in \mathbb{R}_*. \end{cases} \tag{3}$$

Here, $[\![f]\!](t) := f(0^+,t) - f(0^-,t)$ and

$$v_0(x) = \frac{1}{\rho_0(X(x,0))}, \quad u_0(x) = U_0(X(x,0)).$$

We note that (3) does not contain $h(t)$, but we can recover it by $h(t) = h_0 + \int_0^t V(s)\, ds$.

1.2. **Long-time behavior of the point mass: Question of optimality.** In this note, we focus our attention on the long-time behavior of the point mass velocity $V(t)$. In a previous work [4], we showed the decay estimate $V(t) = O(t^{-3/2})$. For a special class of initial data, we even showed that this rate $3/2$ is optimal, that is, no faster decay estimates hold. However, we could not treat general initial data. To enable this is the purpose of the present work.

The main tool we used to prove the decay estimate $V(t) = O(t^{-3/2})$ is the method of pointwise estimates developed in [7, 11]. This method, through a detailed analysis of the fundamental solution to the linearized problem, allows us to prove pointwise estimates of solutions to quasilinear hyperbolic-parabolic systems including the barotropic compressible Navier–Stokes equations. Here, the term *pointwise* means that we obtain inequalities of the form $|f(x,t)| \leq \phi(x,t)$, where f is an unknown and ϕ is an explicit function. Although their works treat the Cauchy problem, we can also analyze initial-boundary value problems by using the Fourier–Laplace transform technique developed in [5, 6]. These methods are applied, for example, to analyze half-space problems of the barotropic compressible Navier–Stokes equations [2]. And in [4], we applied these methods to the free-boundary value problem (3) to show $V(t) = O(t^{-3/2})$.

The necessity to prove pointwise estimates comes from the fact that the L^∞-norm of $(v-1,u)$, where (v,u,V) is the solution to (3), decays as $t^{-1/2}$ in general. This only implies $V(t) = O(t^{-1/2})$, which is far from optimal. By studying the spatial structure of the solution by the method of pointwise estimates, we can show that the solution decays much faster, at least as $t^{-3/2}$, around $x = 0$, and this implies $V(t) = u(0^\pm, t) = O(t^{-3/2})$. Physically, this faster decay around the location of the point mass is due to the compressibility of the fluid, which takes away the $t^{-1/2}$ decaying parts of the solution away from the point mass as sound waves; in contrast, for the fluid governed by viscous Burgers' equation, the point mass velocity $V(t)$ only decays as $t^{-1/2}$ since this fluid lacks compressibility [10]. We also note that the rate $3/2$ comes from the nonlinearity of the Navier–Stokes equations and that $V(t)$ decays exponentially fast if we neglect the nonlinearity.

To tackle the problem of optimality, we refine the pointwise estimates obtained in [4]. Previously, as in [7, 11], we considered an approximation of the solution to (3) by *diffusion waves* — self-similar solutions to generalized Burgers' equations — and obtained error bounds of this approximation in a pointwise manner. Diffusion waves, which decay as $t^{-1/2}$ in the L^∞-norm, provide a leading order approximation of the solution in the L^∞-sense because the approximation error decays at least as $t^{-3/4}$ in the L^∞-norm. However, diffusion waves cannot give the leading order asymptotics of the solution around $x = 0$ since the diffusion waves decay exponentially fast there. Then, in order to understand the long-time behavior of $V(t) = u(0^\pm, t)$ more precisely, a natural question is to find out a leading order approximation of the solution around $x = 0$; we define such waves and dub them *bi-diffusion waves*. This is the line of thought we pursue, and we shall explain this in the next section.

2. Main theorem: Refined pointwise estimates of solutions

In this section, we state the theorem on refined pointwise estimates of the solution to (3). Then, from this theorem, we deduce corollaries on the decay rate of $V(t)$. To state the theorem, we start with some preliminaries.

First, we note that the first two equations in (3), the barotropic compressible Navier–Stokes equations, can be written in vector form as follows:

$$\boldsymbol{u}_t + A\boldsymbol{u}_x = B\boldsymbol{u}_{xx} + \begin{pmatrix} 0 \\ N_x \end{pmatrix}, \tag{4}$$

where

$$\boldsymbol{u} = \begin{pmatrix} v-1 \\ u \end{pmatrix}, \quad A = \begin{pmatrix} 0 & -1 \\ -c^2 & 0 \end{pmatrix}, \quad B = \begin{pmatrix} 0 & 0 \\ 0 & \nu \end{pmatrix}, \quad N = -p(v) + p(1) - c^2(v-1) - \nu\frac{v-1}{v}u_x. \tag{5}$$

Here, $c > 0$ is the speed of sound for the state $(v,u) = (1,0)$ defined by $c^2 = -p'(1)$; for c to be well-defined, we assume that $p'(1) < 0$.[2] The matrix A has two eigenvalues $\lambda_1 = c$ and $\lambda_2 = -c$; as right and left eigenvector of A corresponding to λ_i, we can take r_i and l_i defined by

$$r_1 = \frac{2c}{p''(1)}\begin{pmatrix} -1 \\ c \end{pmatrix}, \quad r_2 = \frac{2c}{p''(1)}\begin{pmatrix} 1 \\ c \end{pmatrix}$$

[2] We consider small solutions around the state $(v,u,V) \equiv (1,0,0)$. The reference volume can be any $v = v_* > 0$, but we set this to unity for simplicity.

and

$$l_1 = \frac{p''(1)}{4c}\begin{pmatrix} -1 & 1/c \end{pmatrix}, \quad l_2 = \frac{p''(1)}{4c}\begin{pmatrix} 1 & 1/c \end{pmatrix}.$$

Here and in what follows, we assume that $p''(1) \neq 0$. We then define u_i $(i = 1, 2)$ as components of $\boldsymbol{u}$ with respect to the basis (r_1, r_2), that is,

$$\boldsymbol{u} = u_1 r_1 + u_2 r_2. \tag{6}$$

Taking into account the relation

$$\begin{pmatrix} l_1 \\ l_2 \end{pmatrix}\begin{pmatrix} r_1 & r_2 \end{pmatrix} = \begin{pmatrix} 1 & 0 \\ 0 & 1 \end{pmatrix},$$

we can calculate u_i by

$$u_i = l_i \boldsymbol{u}. \tag{7}$$

We next define diffusion waves. First, let us write down the i-th component of (4) obtained by multiplying l_i to it:

$$u_{it} + \lambda_i u_{ix} = l_i B \begin{pmatrix} r_1 & r_2 \end{pmatrix}\begin{pmatrix} u_1 \\ u_2 \end{pmatrix}_{xx} + N_{ix} = \frac{\nu}{2}(u_1 + u_2)_{xx} + N_{ix}, \tag{8}$$

where

$$N_i = l_i \begin{pmatrix} 0 \\ N \end{pmatrix} = \frac{p''(1)}{4c^2} N. \tag{9}$$

We note that N_i in fact does not depend on i; we add this subscript just to distinguish N_i from N. By Taylor's theorem, we see that

$$N_i = -\frac{p''(1)^2}{8c^2}(v-1)^2 + O(|v-1|^3) + O(|(v-1)u_x|) = -\frac{1}{2}(-u_1 + u_2)^2 + O(|v-1|^3) + O(|(v-1)u_x|).$$

Now, let $i' = 3 - i$ ($1' = 2$ and $2' = 1$) and neglect terms involving $u_{i'}$ and terms of the order of $O(|v-1|^3)$ and $O(|(v-1)u_x|)$ in (8); then we obtain, writing θ_i instead of u_i,

$$\partial_t \theta_i + \lambda_i \partial_x \theta_i + \partial_x\left(\frac{\theta_i^2}{2}\right) = \frac{\nu}{2}\partial_x^2 \theta_i, \quad x \in \mathbb{R},\ t > 0. \tag{10}$$

In this way, we find a connection between the barotropic Navier–Stokes equations and the generalized Burgers equation (10). Moreover, from the conservation laws

$$\int_{-\infty}^{\infty} u(x,t)\,dx + V(t) = \int_{-\infty}^{\infty} u_0(x)\,dx + V_0, \quad \int_{-\infty}^{\infty} (v-1)(x,t)\,dx = \int_{-\infty}^{\infty} (v_0 - 1)(x)\,dx,$$

we see that

$$\int_{-\infty}^{\infty} u_i(x,t)\,dx + l_i \begin{pmatrix} 0 \\ V(t) \end{pmatrix} = \int_{-\infty}^{\infty} u_{0i}(x)\,dx + l_i \begin{pmatrix} 0 \\ V_0 \end{pmatrix} =: M_i, \tag{11}$$

where

$$u_{0i} = l_i \begin{pmatrix} v_0 - 1 \\ u_0 \end{pmatrix}.$$

Taking this into account, we impose

$$\lim_{t\to -1} \theta_i(x,t) = M_i \delta(x), \tag{12}$$

where $\delta(x)$ is the Dirac delta function. Note that the limit is $\lim_{t\to -1}$ and not $\lim_{t\to 0}$; this is because we don't want θ_i to have singularity at $t = 0$. By the Cole–Hopf transformation, we can solve (10) and (12) explicitly:

$$\theta_i(x,t) = \frac{\sqrt{\nu}}{\sqrt{2(t+1)}} \left(e^{\frac{M_i}{\nu}} - 1\right) e^{-\frac{(x-\lambda_i(t+1))^2}{2\nu(t+1)}} \left[\sqrt{\pi} + \left(e^{\frac{M_i}{\nu}} - 1\right) \int_{\frac{x-\lambda_i(t+1)}{\sqrt{2\nu(t+1)}}}^{\infty} e^{-y^2}\, dy\right]^{-1}.$$

We see from the formula above that θ_i propagates with speed λ_i and spreads like solutions to a diffusion equation; hence we call θ_i the i-th diffusion wave with mass M_i.

Our next task is to define bi-diffusion waves. It requires some detailed calculations to understand the motivation behind their definitions, so we postpone the explanation to Section 3 and give the definitions right away. Let ξ_i be the solution to the following variable coefficient inhomogeneous convective heat equation:

$$\partial_t \xi_i + \lambda_i \partial_x \xi_i + \partial_x(\theta_i \xi_i) + \partial_x \left(\frac{\theta_{i'}^2}{2}\right) = \frac{\nu}{2} \partial_x^2 \xi_i, \quad x \in \mathbb{R}, t > 0 \tag{13}$$

with

$$\xi_i(x,0) = 0, \quad x \in \mathbb{R}. \tag{14}$$

Here, we remind that $i' = 3 - i$. We call ξ_i the i-th bi-diffusion wave with mass pair (M_1, M_2). In Figure 2, we show graphs of ξ_i. The figure visually explains the reason why we call it a bi-diffusion wave.

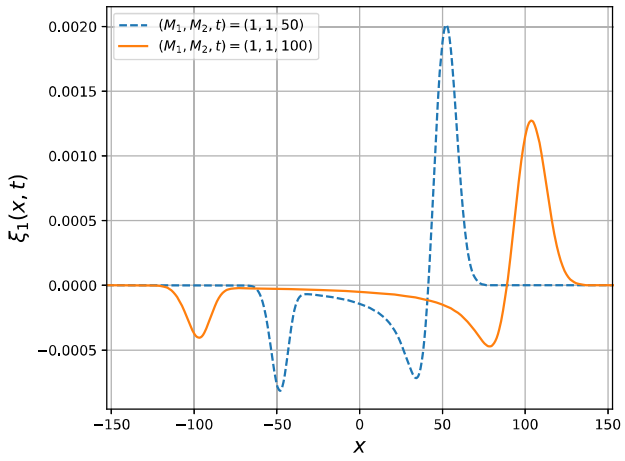

FIGURE 2. In this figure, we set $c = 1$, $\nu = 1$, and $(M_1, M_2) = (1, 1)$. The dotted and solid line represent ξ_1 at time $t = 50$ and $t = 100$, respectively. We can see that the wave spreads in both directions although the right part is more dominant.

We add few more notations to state the theorem. First, let

$$\psi_{7/4}(x,t;\lambda_i) = [(x-\lambda_i(t+1))^2 + (t+1)]^{-7/8},$$
$$\bar{\psi}(x,t;\lambda_i) = [|x-\lambda_i(t+1)|^7 + (t+1)^5]^{-1/4},$$

and

$$\Psi_i(x,t) = \psi_{7/4}(x,t;\lambda_i) + \bar{\psi}(x,t;\lambda_{i'}). \tag{15}$$

An important property of Ψ_i is that $\Psi_i(0,t) = O(t^{-7/4})$ (note that $7/4 > 3/2$). We also have $\Psi_i(\lambda_i t, t) = O(t^{-7/8})$ and $\Psi_i(\lambda_{i'} t, t) = O(t^{-5/4})$. Secondly, let

$$C_1(v,u) := -p(v) + \nu\frac{u_x}{v},$$
$$C_2(v,u) := -p'(v)u_x + \frac{\nu}{v}\left(-p(v) + \nu\frac{u_x}{v}\right)_{xx} - \nu\frac{u_x^2}{v^2}.$$

We note that if (v,u,V) is the solution to (3), then $C_2(v,u) = \partial_t C_1(v,u)$. Next, we introduce

$$u_{0i}^-(x) := \int_{-\infty}^{x} u_{0i}(y)\,dy, \quad u_{0i}^+(x) := \int_{x}^{\infty} u_{0i}(y)\,dy. \tag{16}$$

Finally, let $[\![f]\!] := f(0^+) - f(0^-)$ and denote by $||\cdot||_k$ ($k \in \mathbb{N}$) the Sobolev $H^k(\mathbb{R}_*)$-norm.

Our main theorem reads as follows.

Theorem 2.1. *Let $v_0 - 1, u_0 \in H^6(\mathbb{R}_*)$ and $V_0 \in \mathbb{R}$. Assume that they satisfy the following compatibility conditions:*

$$u_0(0^\pm) = V_0, \quad C_1(v_0,u_0)_x(0^\pm) = [\![C_1(v_0,u_0)]\!], \quad C_2(v_0,u_0)_x(0^\pm) = [\![C_2(v_0,u_0)]\!].$$

Under these assumptions, there exist $\delta_0, C > 0$ such that if

$$\delta := \sum_{i=1}^{2}\left[||u_{0i}||_6 + \sup_{x\in\mathbb{R}^*}\left\{(|x|+1)^{7/4}|u_{0i}(x)|\right\} + \sup_{x>0}\left\{(|x|+1)^{5/4}(|u_{0i}^-(-x)| + |u_{0i}^+(x)|)\right\}\right] \le \delta_0, \tag{17}$$

then the unique global-in-time solution (v,u,V) to (3) satisfies the pointwise estimates

$$|(u_i - \theta_i - \xi_i - \gamma_{i'}\partial_x\theta_{i'})(x,t)| \le C\delta\Psi_i(x,t) \quad (x \in \mathbb{R}_*, t \ge 0; i = 1,2), \tag{18}$$

where $i' = 3 - i$ and $\gamma_i = (-1)^i\nu/(4c)$.

We add some remarks.

(i) We have not mentioned any result on the existence of solutions; for this, see [3, Theorem 2.1].

(ii) The decay rates of functions appearing in (18) are as follows: (I) In the $O(1)$-neighborhood of $x = \lambda_i t$, we have $\theta_i(x,t) = O(t^{-1/2})$, $\xi_i(x,t) = O(t^{-3/4})$, $\partial_x\theta_{i'}(x,t) = O(e^{-t/C})$, and $\Psi_i(x,t) = O(t^{-7/8})$. (II) In the $O(1)$-neighborhood of $x = 0$, we have $\theta_i(x,t) = O(e^{-t/C})$, $\xi_i(x,t) = O(t^{-3/2})$, $\partial_x\theta_{i'}(x,t) = O(e^{-t/C})$, and $\Psi_i(x,t) = O(t^{-7/4})$. (III) In the-$O(1)$ neighborhood of $x = \lambda_{i'}t$, we have $\theta_i(x,t) = O(e^{-t/C})$, $\xi_i(x,t) = O(t^{-1})$, $\partial_x\theta_{i'}(x,t) = O(t^{-1})$, and $\Psi_i(x,t) = O(t^{-5/4})$. Hence, around $x = \lambda_i t$, the leading order term is θ_i, and the second order term is ξ_i; around $x = 0$, the leading order term is ξ_i; around $x = \lambda_{i'}t$, the leading order terms are ξ_i and $\gamma_{i'}\partial_x\theta_{i'}$.

(iii) In the previous work [4], we obtained pointwise estimates for $u_i - \theta_i$. From (iii) above, we then lose the information on the leading order asymptotics of $V(t) = u(0^\pm, t)$.

By Theorem 2.1, we have

$$V(t) = u(0^{\pm}, t) = \frac{2c^2}{p''(1)}(u_1 + u_2)(0^{\pm}, t) = \frac{2c^2}{p''(1)}(\xi_1 + \xi_2)(0, t) + O(t^{-7/4}).$$

From this, we obtain two Corollaries on the long-time behavior of $V(t)$.

Corollary 2.1. *Define M_i by (11) and assume that $(M_1 + M_2)(M_1 - M_2) \neq 0$, that is,*

$$\left[\int_{-\infty}^{\infty} (v_0 - 1)(x)\, dx\right] \cdot \left[\int_{-\infty}^{\infty} u_0(x)\, dx + V_0\right] \neq 0.$$

Then under the assumptions of Theorem 2.1, there exist $\delta_0 > 0$, $C > 1$, and $T(\delta) > 0$ such that if (17) holds, then the solution (v, u, V) to (3) satisfies

$$C^{-1}|M_1^2 - M_2^2|(t+1)^{-3/2} \leq \operatorname{sgn}(M_1^2 - M_2^2)V(t) \quad (t \geq T(\delta)).$$

In particular, this implies

$$C^{-1}|M_1^2 - M_2^2|(t+1)^{-3/2} \leq |V(t)| \quad (t \geq T(\delta)).$$

Corollary 2.2. *Define M_i by (11) and assume that $(M_1 + M_2)(M_1 - M_2) = 0$, that is,*

$$\left[\int_{-\infty}^{\infty} (v_0 - 1)(x)\, dx\right] \cdot \left[\int_{-\infty}^{\infty} u_0(x)\, dx + V_0\right] = 0.$$

Then under the assumptions of Theorem 2.1, there exist $\delta_0, C > 0$ such that if (17) holds, then the solution (v, u, V) to (3) satisfies

$$|V(t)| \leq C\delta(t+1)^{-7/4} \quad (t \geq 0).$$

Again, we add some remarks.

(i) From the two Corollaries above, we can conclude that the condition $(M_1+M_2)(M_1-M_2) \neq 0$ is a necessarily and sufficient condition for the optimality of the decay estimate $V(t) = O(t^{-3/2})$. When $(M_1 + M_2)(M_1 - M_2) \neq 0$, we can even predict that the final sign of $V(t)$ is $M_1^2 - M_2^2$.

(ii) By (2), we can check that

$$\int_{-\infty}^{\infty} (v_0 - 1)(x)\, dx = -\int_{-\infty}^{\infty} (\rho_0 - 1)(X)\, dX, \quad \int_{-\infty}^{\infty} u_0(x)\, dx = \int_{-\infty}^{\infty} (\rho_0 U_0)(X)\, dX.$$

Therefore, the condition $(M_1 + M_2)(M_1 - M_2) \neq 0$ means that the initial perturbations of the density and the momentum are both non-zero.

(iii) To deduce the corollaries above from Theorem 2.1, we need to analyze the long-time behavior of $\xi_i(0, t)$. Corollary 2.1 is not so difficult to prove. On the other hand, the proof of Corollary 2.2 is not so straightforward and requires some care.

(iv) We can also ask whether the decay estimate $V(t) = O(t^{-7/4})$ is optimal under the constraint $(M_1 + M_2)(M_1 - M_2) = 0$. We have not proved this mathematically. However, this seems to be true. See Section 4 for a numerical evidence.

We can also obtain similar results for the Cauchy problem:

$$\begin{cases} v_t - u_x = 0, & x \in \mathbb{R},\ t > 0, \\ u_t + p(v)_x = \nu\left(\dfrac{u_x}{v}\right)_x, & x \in \mathbb{R},\ t > 0, \\ v(x, 0) = v_0(x),\ u(x, 0) = u_0(x), & x \in \mathbb{R}. \end{cases} \tag{19}$$

Theorem 2.2. *Let $v_0 - 1, u_0 \in H^6(\mathbb{R})$, and define M_i by*

$$M_i := \int_{-\infty}^{\infty} u_{0i}(x)\,dx \tag{20}$$

instead of (11). Under this setting, there exist $\delta_0, C > 0$ such that if

$$\delta := \sum_{i=1}^{2}\left[\|u_{0i}\|_6 + \sup_{x\in\mathbb{R}}\left\{(|x|+1)^{7/4}|u_{0i}(x)|\right\} + \sup_{x\geq 0}\left\{(|x|+1)^{5/4}(|u_{0i}^-(-x)| + |u_{0i}^+(x)|)\right\}\right] \leq \delta_0, \tag{21}$$

then the unique global-in-time solution (v,u) to (19) satisfies the pointwise estimates

$$|(u_i - \theta_i - \xi_i - \gamma_{i'}\partial_x\theta_{i'})(x,t)| \leq C\delta\Psi_i(x,t) \quad (x\in\mathbb{R}, t\geq 0; i = 1,2),$$

where $i' = 3 - i$ and $\gamma_i = (-1)^i\nu/(4c)$.

Corollary 2.3. *Define M_i by (20) and assume that $(M_1+M_2)(M_1-M_2)\neq 0$, that is,*

$$\left[\int_{-\infty}^{\infty}(v_0-1)(x)\,dx\right]\cdot\left[\int_{-\infty}^{\infty}u_0(x)\,dx\right]\neq 0.$$

Then under the assumptions of Theorem 2.2, there exist $\delta_0 > 0$, $C > 1$, and $T(\delta) > 0$ such that if (21) holds, then the solution (v,u) to (19) satisfies

$$C^{-1}|M_1^2 - M_2^2|(t+1)^{-3/2} \leq \operatorname{sgn}(M_1^2 - M_2^2)u(0,t) \quad (t\geq T(\delta)).$$

In particular, this implies

$$C^{-1}|M_1^2 - M_2^2|(t+1)^{-3/2} \leq |u(0,t)| \quad (t\geq T(\delta)).$$

Corollary 2.4. *Define M_i by (20) and assume that $(M_1+M_2)(M_1-M_2) = 0$, that is,*

$$\left[\int_{-\infty}^{\infty}(v_0-1)(x)\,dx\right]\cdot\left[\int_{-\infty}^{\infty}u_0(x)\,dx\right] = 0.$$

Then under the assumptions of Theorem 2.2, there exist $\delta_0, C > 0$ such that if (21) holds, then the solution (v,u) to (19) satisfies

$$|u(0,t)| \leq C\delta(t+1)^{-7/4} \quad (t\geq 0).$$

3. Idea of the proof

In this section, we explain the idea of the proof of Theorem 2.2 for the Cauchy problem; combining the techniques developed in [4], we can prove Theorem 2.1 in a similar manner. We shall explain the idea of the proof somewhat heuristically rather than to show the details of the calculations; the focal point of our exposition is to explain the origin of the bi-diffusion wave ξ_i.

The proof starts by writing an integral equation for the solution to (19) in terms of the fundamental solution to the linearized problem.

3.1. **Integral equation.** We define the fundamental solution $G = G(x,t) \in \mathbb{R}^{2\times 2}$ to the linearized problem of (19) by

$$\begin{cases} \partial_t G + \begin{pmatrix} 0 & -1 \\ -c^2 & 0 \end{pmatrix} \partial_x G = \begin{pmatrix} 0 & 0 \\ 0 & \nu \end{pmatrix} \partial_x^2 G, & x \in \mathbb{R},\ t > 0, \\ G(x,0) = \delta(x) \begin{pmatrix} 1 & 0 \\ 0 & 1 \end{pmatrix}, & x \in \mathbb{R}, \end{cases}$$

where $\delta(x)$ is the Dirac delta function. Then, by applying Duhamel's principle to (4), we obtain the following.

Proposition 3.1. *The solution (v,u) to (19) satisfies the following integral equation:*

$$\begin{aligned} \begin{pmatrix} v-1 \\ u \end{pmatrix}(x,t) &= \int_{-\infty}^{\infty} G(x-y,t) \begin{pmatrix} v_0 - 1 \\ u_0 \end{pmatrix}(y)\, dy \\ &\quad + \int_0^t \int_{-\infty}^{\infty} G(x-y,t-s) \begin{pmatrix} 0 \\ N_x \end{pmatrix}(y,s)\, dyds. \end{aligned} \tag{22}$$

To write down the corresponding integral equation for u_i defined by (7), we introduce

$$g_i := l_i G \begin{pmatrix} r_1 & r_2 \end{pmatrix}.$$

Then, by multiplying l_i to (22) and using

$$\begin{pmatrix} v_0 - 1 \\ u_0 \end{pmatrix} = \begin{pmatrix} r_1 & r_2 \end{pmatrix} \begin{pmatrix} u_{01} \\ u_{02} \end{pmatrix}, \quad \begin{pmatrix} 0 \\ N \end{pmatrix} = \begin{pmatrix} r_1 & r_2 \end{pmatrix} \begin{pmatrix} N_1 \\ N_2 \end{pmatrix},$$

we obtain

$$u_i(x,t) = \int_{-\infty}^{\infty} g_i(x-y,t) \begin{pmatrix} u_{01} \\ u_{02} \end{pmatrix}(y)\, dy + \int_0^t \int_{-\infty}^{\infty} g_i(x-y,t-s) \begin{pmatrix} N_1 \\ N_2 \end{pmatrix}_x (y,s)\, dyds. \tag{23}$$

3.2. **Pointwise estimates of the fundamental solution.** To analyze (23), we need the pointwise estimates of the fundamental solution G proved in [8]. First, define $G^* = G^*(x,t) \in \mathbb{R}^{2\times 2}$ by

$$G^*(x,t) = \frac{1}{2(2\pi\nu t)^{1/2}} e^{-\frac{(x-ct)^2}{2\nu t}} \begin{pmatrix} 1 & -\frac{1}{c} \\ -c & 1 \end{pmatrix} + \frac{1}{2(2\pi\nu t)^{1/2}} e^{-\frac{(x+ct)^2}{2\nu t}} \begin{pmatrix} 1 & \frac{1}{c} \\ c & 1 \end{pmatrix}.$$

Then, for any integer $k \geq 0$, the following pointwise estimates hold [8, Theorem 1.3]:

$$\begin{aligned} &\partial_x^k G(x,t) - \partial_x^k G^*(x,t) \\ &\quad - \gamma_1 \partial_x^{k+1} \frac{e^{-\frac{(x-ct)^2}{2\nu t}}}{(2\pi\nu t)^{1/2}} \begin{pmatrix} -1 & 0 \\ 0 & 1 \end{pmatrix} - \gamma_2 \partial_x^{k+1} \frac{e^{-\frac{(x+ct)^2}{2\nu t}}}{(2\pi\nu t)^{1/2}} \begin{pmatrix} -1 & 0 \\ 0 & 1 \end{pmatrix} - e^{-\frac{c^2}{\nu}t} \sum_{j=0}^{k} \delta^{(k-j)}(x) Q_j(t) \\ &= O(1)(t+1)^{-1/2} t^{-\frac{k+1}{2}} e^{-\frac{(x-ct)^2}{Ct}} \begin{pmatrix} 1 & -\frac{1}{c} \\ -c & 1 \end{pmatrix} + O(1)(t+1)^{-1/2} t^{-\frac{k+1}{2}} e^{-\frac{(x+ct)^2}{Ct}} \begin{pmatrix} 1 & \frac{1}{c} \\ c & 1 \end{pmatrix} \\ &\quad + O(1)(t+1)^{-1/2} t^{-\frac{k+2}{2}} \left(e^{-\frac{(x-ct)^2}{Ct}} + e^{-\frac{(x+ct)^2}{Ct}} \right). \end{aligned} \tag{24}$$

Here, $\gamma_i = (-1)^i \nu/(4c)$, $O(1)$ denotes a scalar function $f(x,t)$ satisfying $|f(x,t)| \leq C$, $\delta^{(k)}(x)$ is the k-th derivative of the Dirac delta function, and $Q_j = Q_j(t)$ is a 2×2 polynomial matrix. Additionally,

we have

$$Q_0 = \begin{pmatrix} 1 & 0 \\ 0 & 0 \end{pmatrix}, \quad Q_1 = \begin{pmatrix} 0 & -\frac{1}{\nu} \\ -\frac{c^2}{\nu} & 0 \end{pmatrix}.$$

For small t, we rather use the following pointwise estimates obtained in [11]:

$$\left| \partial_x^k G(x,t) - \partial_x^k G^*(x,t) - e^{-\frac{c^2}{\nu}t} \sum_{j=0}^{k} \delta^{(k-j)}(x) Q_j(t) \right| \le C(t+1)^{-\frac{1}{2}} t^{-\frac{k+1}{2}} \left(e^{-\frac{(x-ct)^2}{Ct}} + e^{-\frac{(x+ct)^2}{Ct}} \right). \tag{25}$$

We note that in the previous work [4], we only used (25); in the present work, we also need (24).

We finally note that if we set

$$g_i^* := l_i G^* \begin{pmatrix} r_1 & r_2 \end{pmatrix},$$

then we have

$$g_1^* = \begin{pmatrix} g_{11}^* & 0 \end{pmatrix} = \frac{1}{(2\pi\nu t)^{1/2}} e^{-\frac{(x-ct)^2}{2\nu t}} \begin{pmatrix} 1 & 0 \end{pmatrix}, \quad g_2^* = \begin{pmatrix} 0 & g_{22}^* \end{pmatrix} = \frac{1}{(2\pi\nu t)^{1/2}} e^{-\frac{(x+ct)^2}{2\nu t}} \begin{pmatrix} 0 & 1 \end{pmatrix}.$$

3.3. **Origin of ξ_i and $\gamma_{i'}\partial_x\theta_{i'}$: A heuristic argument.** Our aim here is to find an appropriate function $w_i = w_i(x,t)$ such that, if we set

$$v_i = u_i - w_i,$$

then the following pointwise estimates hold:

$$|v_i(x,t)| \le C\delta\Psi_i(x,t) \quad (x \in \mathbb{R}, t \ge 0; i = 1,2). \tag{26}$$

It turns out that $w_i = \theta_i + \xi_i + \gamma_{i'}\partial_x\theta_{i'}$ will do the work. Here, we try to heuristically justify this choice, thus revealing the origin of ξ_i and $\gamma_{i'}\partial_x\theta_{i'}$. This, we hope, helps the reader go through the detailed but somewhat long calculations in [3].

We first try the choice $w_i = \theta_i$, and hence $v_i = u_i - \theta_i$. Such initial guess is not absurd. In fact, as we mentioned earlier, neglecting terms involving $u_{i'}$ and higher order terms in (8) leads to (10). Now, since (24) implies that the leading order asymptotics of g_i is given by g_i^*, we approximate (23) as follows:

$$\begin{aligned} u_i(x,t) &\sim \int_{-\infty}^{\infty} g_i^*(x-y,t) \begin{pmatrix} u_{01} \\ u_{02} \end{pmatrix}(y)\, dy + \int_0^t \int_{-\infty}^{\infty} g_i^*(x-y,t-s) \begin{pmatrix} N_1 \\ N_2 \end{pmatrix}_x (y,s)\, dyds \\ &= \int_{-\infty}^{\infty} g_{ii}^*(x-y,t) u_{0i}(y)\, dy + \int_0^t \int_{-\infty}^{\infty} g_{ii}^*(x-y,t-s) N_{ix}(y,s)\, dyds. \end{aligned} \tag{27}$$

Here and in what follows, without giving a precise definition, we write $f \sim g$ if the long-time behavior of f and g are similar. Since θ_i satisfies the integral equation

$$\theta_i(x,t) = \int_{-\infty}^{\infty} g_{ii}^*(x-y,t)\theta_i(y,0)\, dy - \int_0^t \int_{-\infty}^{\infty} g_{ii}^*(x-y,t-s) \left(\frac{\theta_i^2}{2} \right)_x (y,s)\, dyds, \tag{28}$$

we obtain

$$
\begin{aligned}
v_i(x,t) \sim & \int_{-\infty}^{\infty} g_{ii}^*(x-y,t)(u_i-\theta_i)(y,0)\,dy \\
& + \int_0^t \int_{-\infty}^{\infty} g_{ii}^*(x-y,t-s)\left(N_i + \frac{\theta_i^2}{2}\right)_x (y,s)\,dyds.
\end{aligned} \tag{29}
$$

For the term related to the initial data, we note that, by (10), (12), and (20),

$$
\int_{-\infty}^{\infty} (u_i-\theta_i)(x,0)\,dx = 0.
$$

Therefore, the anti-derivative $\int_{-\infty}^{x}(u_i-\theta_i)(y,0)\,dy$ of $(u_i-\theta_i)(x,0)$ decays at spatially infinity.[3] Then, we can gain time decay by integration by parts since $\partial_x g_{ii}^*$ decays faster than g_{ii}^*. For the term related to N_i, by (5), (6), and (9), we have

$$
\begin{aligned}
N_i &= -\frac{p''(1)^2}{8c^2}(v-1)^2 + O(|v-1|^3) + O(|(v-1)u_x|) \\
&\sim -\frac{p''(1)^2}{8c^2}(v-1)^2 = -\frac{1}{2}(-\theta_1 - v_1 + \theta_2 + v_2)^2 \\
&\sim -\frac{1}{2}\theta_1^2 - \frac{1}{2}\theta_2^2 + (-\theta_1+\theta_2)v_1 + (\theta_1-\theta_2)v_2 - \frac{1}{2}(-v_1+v_2)^2.
\end{aligned} \tag{30}
$$

Here, we neglected $\theta_1\theta_2$ since it decays exponentially fast. Hence, we have

$$
N_i + \frac{\theta_i^2}{2} \sim -\frac{1}{2}\theta_{i'}^2 + (-\theta_1+\theta_2)v_1 + (\theta_1-\theta_2)v_2 - \frac{1}{2}(-v_1+v_2)^2.
$$

Let us set aside for the moment the terms involving v_i. Then, the nonlinear term in (29) is principally

$$
\zeta_i(x,t) := -\int_0^t \int_{-\infty}^{\infty} g_{ii}^*(x-y,t-s)\left(\frac{\theta_{i'}^2}{2}\right)_x (y,s)\,dyds. \tag{31}
$$

It turns out, however, that this term cannot be bounded by the right-hand side of (26). Therefore, the choice $w_i = \theta_i$ is not enough.

From the analysis above, we improve our guess by taking $w_i = \theta_i + \zeta_i$. Setting $v_i = u_i - \theta_i - \zeta_i$, we have, by (27), (28), and (31),

$$
\begin{aligned}
v_i(x,t) \sim & \int_{-\infty}^{\infty} g_{ii}^*(x-y,t)(u_i-\theta_i)(y,0)\,dy \\
& + \int_0^t \int_{-\infty}^{\infty} g_{ii}^*(x-y,t-s)\left(N_i + \frac{\theta_1^2+\theta_2^2}{2}\right)_x (y,s)\,dyds.
\end{aligned} \tag{32}
$$

[3] The use of this anti-derivative explains the reason why we needed to introduce $u_{0i}^{\pm}$; see (16).

Similar to (30), we have

$$\begin{aligned} N_i &\sim -\frac{p''(1)^2}{8c^2}(v-1)^2 = -\frac{1}{2}(-\theta_1-\zeta_1-v_1+\theta_2+\zeta_2+v_2)^2 \\ &= -\frac{1}{2}\theta_1^2 - \frac{1}{2}\theta_2^2 - \theta_1\zeta_1 - \theta_2\zeta_2 \\ &\quad -\frac{1}{2}\zeta_1^2 - \frac{1}{2}\zeta_2^2 + \theta_1\theta_2 + \theta_1\zeta_2 + \zeta_1\theta_2 + \zeta_1\zeta_2 \\ &\quad + (-\theta_1-\zeta_1+\theta_2+\zeta_2)v_1 + (\theta_1+\zeta_1-\theta_2-\zeta_2)v_2 - \frac{1}{2}(-v_1+v_2)^2. \end{aligned}$$

Hence, we have

$$N_i + \frac{\theta_1^2+\theta_2^2}{2} \sim -\theta_1\zeta_1 - \theta_2\zeta_2 + (-\theta_1-\zeta_1+\theta_2+\zeta_2)v_1 + (\theta_1+\zeta_1-\theta_2-\zeta_2)v_2 - \frac{1}{2}(-v_1+v_2)^2.$$

Here, we neglected terms that are less important than $\theta_i\zeta_i$. Again, let us set aside for the moment the terms involving v_i. Then, the nonlinear term in (32) is principally the sum of

$$\eta_i^{(1)}(x,t) := -\int_0^t \int_{-\infty}^{\infty} g_{ii}^*(x-y,t-s)(\theta_i\zeta_i)_x(y,s)\,dyds \tag{33}$$

and

$$-\int_0^t \int_{-\infty}^{\infty} g_{ii}^*(x-y,t-s)(\theta_{i'}\zeta_{i'})_x(y,s)\,dyds.$$

However, the latter term is less important compared to $\eta_i^{(1)}$; to show this, we need to make use of the differential equation satisfied by ζ_i (see (35) below and [3, Lemma C.1]). For $\eta_i^{(1)}$, it turns out that it cannot be bounded by the right-hand side of (26). Therefore, the choice $w_i = \theta_i + \zeta_i$ is again not enough.

We now repeat the argument above with the choice $w_i = \theta_i + \zeta_i + \eta_i^{(1)}$. Then, we find that we need to add

$$\eta_i^{(2)}(x,t) := -\int_0^t \int_{-\infty}^{\infty} g_{ii}^*(x-y,t-s)\left(\theta_i\eta_i^{(1)}\right)_x(y,s)\,dyds$$

to w_i, that is, we upgrade the guess to $w_i = \theta_i + \zeta_i + \eta_i^{(1)} + \eta_i^{(2)}$. Repeating this, we come to define $\eta_i^{(n)}$ inductively by

$$\eta_i^{(n)}(x,t) := -\int_0^t \int_{-\infty}^{\infty} g_{ii}^*(x-y,t-s)\left(\theta_i\eta_i^{(n-1)}\right)_x(y,s)\,dyds \quad (n\geq 2), \tag{34}$$

and set $w_i = \theta_i + \zeta_i + \sum_{n=1}^{\infty}\eta_i^{(n)}$. By (31), (33), and (34), we see that ζ_i and $\eta_i^{(n)}$ satisfy

$$\begin{cases} \partial_t\zeta_i + \lambda_i\partial_x\zeta_i + \partial_x\left(\dfrac{\theta_{i'}^2}{2}\right) = \dfrac{\nu}{2}\partial_x^2\zeta_i, & x\in\mathbb{R}, t>0, \\ \zeta_i(x,0) = 0, & x\in\mathbb{R}, \end{cases} \tag{35}$$

$$\begin{cases} \partial_t\eta_i^{(1)} + \lambda_i\partial_x\eta_i^{(1)} + \partial_x(\theta_i\zeta_i) = \dfrac{\nu}{2}\partial_x^2\eta_i^{(1)}, & x\in\mathbb{R}, t>0, \\ \eta_i^{(1)}(x,0) = 0, & x\in\mathbb{R}, \end{cases}$$

and

$$\begin{cases} \partial_t \eta_i^{(n)} + \lambda_i \partial_x \eta_i^{(n)} + \partial_x \left(\theta_i \eta_i^{(n-1)} \right) = \dfrac{\nu}{2} \partial_x^2 \eta_i^{(n)}, & x \in \mathbb{R}, t > 0, \\ \eta_i^{(n)}(x,0) = 0, & x \in \mathbb{R} \end{cases}$$

for $n \geq 2$. Summing these up, we see that $\Xi_i := \zeta_i + \sum_{n=1}^{\infty} \eta_i^{(n)}$ satisfies

$$\begin{cases} \partial_t \Xi_i + \lambda_i \partial_x \Xi_i + \partial_x (\theta_i \Xi_i) + \partial_x \left(\dfrac{\theta_{i'}^2}{2} \right) = \dfrac{\nu}{2} \partial_x^2 \xi_i, & x \in \mathbb{R}, t > 0, \\ \Xi_i(x,0) = 0, & x \in \mathbb{R}. \end{cases}$$

Hence, by (13) and (14), we conclude that $\Xi_i = \xi_i$.

We are almost done. But we also need to add $\gamma_{i'} \partial_x \theta_{i'}$ to w_i. This can be explained as follows. By (24), the right-hand side of (23) contains

$$\begin{aligned} &\gamma_{i'} \int_{-\infty}^{\infty} \left\{ \partial_x \frac{e^{-\frac{(x-\lambda_{i'}t)^2}{2\nu t}}}{(2\pi\nu t)^{1/2}} \right\} C_i \begin{pmatrix} u_{01} \\ u_{02} \end{pmatrix} (y)\, dy \\ &+ \gamma_{i'} \int_0^t \int_{-\infty}^{\infty} \left\{ \partial_x \frac{e^{-\frac{(x-\lambda_{i'}(t-s))^2}{2\nu(t-s)}}}{(2\pi\nu(t-s))^{1/2}} \right\} C_i \begin{pmatrix} N_1 \\ N_2 \end{pmatrix}_x (y,s)\, dyds, \end{aligned} \tag{36}$$

where

$$C_i = l_i \begin{pmatrix} -1 & 0 \\ 0 & 1 \end{pmatrix} \begin{pmatrix} r_1 & r_2 \end{pmatrix} = \begin{pmatrix} \delta_{i2} & \delta_{i1} \end{pmatrix}.$$

Here, δ_{lm} is the Kronecker delta. As we saw in (30), N_i contains the quadratic term $-\theta_{i'}^2/2$. Therefore, (36) contains

$$\gamma_{i'} \int_{-\infty}^{\infty} \left\{ \partial_x \frac{e^{-\frac{(x-\lambda_{i'}t)^2}{2\nu t}}}{(2\pi\nu t)^{1/2}} \right\} u_{0i'}(y)\, dy - \gamma_{i'} \int_0^t \int_{-\infty}^{\infty} \left\{ \partial_x \frac{e^{-\frac{(x-\lambda_{i'}(t-s))^2}{2\nu(t-s)}}}{(2\pi\nu(t-s))^{1/2}} \right\} \left(\frac{\theta_{i'}^2}{2} \right)_x (y,s)\, dyds.$$

It is not difficult to see that this term is well approximated by $\gamma_{i'} \partial_x \theta_{i'}$. This explains the choice $w_i = \theta_i + \xi_i + \gamma_{i'} \partial_x \theta_{i'}$.

3.4. **Estimates of the nonlinear terms.** We now explain the final step of the proof. We set $v_i = u_i - (\theta_i + \xi_i + \gamma_{i'} \partial_x \theta_{i'})$. Since we already have the integral equations for u_i, θ_i, and ξ_i, we can write down an integral equation for v_i.

What we now do is this. We set

$$P(t) := \sum_{i=1}^{2} \sup_{0 \leq s \leq t} |v_i(\cdot, s) \Psi_i(\cdot, s)^{-1}|_\infty.$$

Here, Ψ_i is defined by (15) and $|\cdot|_\infty$ is the $L^\infty(\mathbb{R}_*)$-norm.[4] We then have

$$|v_i(x,t)| \leq P(t) \Psi_i(x,t) \quad (x \in \mathbb{R}, t \geq 0; i = 1,2).$$

[4]It should be noted that we do not know a priori that $P(t)$ is finite, but we do not go into this problem here.

Using this, we estimate all the terms appearing in the integral equation for v_i to show

$$P(t) \le C\delta + C(\delta + P(t))^2 \quad (t \ge 0).$$

Here, δ is defined by (21) and C is a positive constant independent of t. From this, by a standard argument, it follows that if δ is sufficiently small, there exists a positive constant C' independent of t such that $P(t) \le C'\delta$ for all $t \ge 0$. We then conclude that

$$|v_i(x,t)| \le P(t)\Psi_i(x,t) \le C'\Psi_i(x,t) \quad (x \in \mathbb{R}, t \ge 0; i = 1,2),$$

which is what we wanted to prove.

Now, it remains to bound numerous convolutions of functions appearing in the integral equation for v_i. The required calculations are long, and these are done in [3]. We omitted this core calculations, but we now at least know the heart of the proof.

4. Numerical validation of mathematical results

In this section, we present numerical simulations that support the results in Section 2. To avoid difficulties related to the treatment of the boundary, we consider the Cauchy problem (19) with the ideal gas law $p(v) = 1/v$ and numerically validate Corollaries 2.3 and 2.4. In this section, we set $\nu = 1$.

4.1. **Pseudospectral scheme.**

We use a pseudospectral method (cf. [1]) to numerically simulate (19). We describe the scheme below.

Since (19) is posed on the whole space $\mathbb{R}$, we take $L > 0$ large enough and consider instead the following equations:

$$\begin{cases} v_t - u_x = 0, & x \in (-L, L),\ t > 0, \\ u_t + p(v)_x = \left(\dfrac{u_x}{v}\right)_x, & x \in (-L, L),\ t > 0, \\ v(-L,t) = v(L,t),\ u(-L,t) = u(L,t), & t > 0, \\ v(x,0) = v_0(x),\ u(x,0) = u_0(x), & x \in (-L, L). \end{cases} \tag{37}$$

Here, we impose periodic boundary conditions, and we expect that if L is large enough, the solution to (37) should give an approximation of the solution to (19); the effect of the finiteness of the domain should be assessed by varying L in a certain range.[5] Moreover, to make the domain L-independent, we change the variables as follows:

$$y = \frac{\pi}{L}x, \quad \tilde{v}(y,t) = v(x,t), \quad \tilde{u}(y,t) = u(x,t).$$

Then, after replacing the symbols $(\tilde{v}, \tilde{u})$ by (v, u), (37) becomes

$$\begin{cases} v_t - \alpha_L u_y = 0, & y \in (-\pi, \pi),\ t > 0, \\ u_t + \alpha_L p(v)_y = \alpha_L^2 \left(\dfrac{u_y}{v}\right)_y, & y \in (-\pi, \pi),\ t > 0, \\ v(-\pi,t) = v(\pi,t),\ u(-\pi,t) = u(\pi,t), & t > 0, \\ v(y,0) = v_0(y/\alpha_L),\ u(y,0) = u_0(y/\alpha_L), & y \in (-\pi, \pi), \end{cases} \tag{38}$$

[5] When we consider initial data localized around the origin, $L = 2cT = 2T$ is usually large enough (T is the maximum simulation time).

where $\alpha_L = \pi/L$.

Spectral methods use discrete Fourier transforms to approximate solutions to differential equations. In our case, this means that we seek an approximation of the solution (v, u) to (38) in the form

$$v^n(y,t) = \frac{1}{n}\sum_{k=-n/2}^{n/2-1}(-1)^k \hat{v}_k^n(t)\exp(\sqrt{-1}ky), \quad u^n(y,t) = \frac{1}{n}\sum_{k=-n/2}^{n/2-1}(-1)^k \hat{u}_k^n(t)\exp(\sqrt{-1}ky) \tag{39}$$

with sufficiently large n (an even positive integer). The task now is to determine the Fourier coefficients $\{\hat{v}_k^n(t), \hat{u}_k^n(t)\}$ properly so that (v^n, u^n) approximately satisfies (37). Concerning the initial condition, we use the following fact: if we set

$$\begin{cases} v_j^n(t) := v^n(y_j,t) = \dfrac{1}{n}\displaystyle\sum_{k=-n/2}^{n/2-1}\hat{v}_k^n(t)\exp(2\pi\sqrt{-1}jk/n), & j = 0,1,\dots,n-1, \\ u_j^n(t) := u^n(y_j,t) = \dfrac{1}{n}\displaystyle\sum_{k=-n/2}^{n/2-1}\hat{u}_k^n(t)\exp(2\pi\sqrt{-1}jk/n), & j = 0,1,\dots,n-1, \end{cases}$$

where

$$y_j = 2\pi\frac{j-n/2}{n},$$

then we have

$$\hat{v}_k^n(t) = \sum_{j=0}^{n-1} v_j^n(t)\exp(-2\pi\sqrt{-1}jk/n), \quad \hat{u}_k^n(t) = \sum_{j=0}^{n-1} u_j^n(t)\exp(-2\pi\sqrt{-1}jk/n).^{6}$$

Hence, it is natural to set

$$\hat{v}_k^n(0) = \sum_{j=0}^{n-1} v_0(y_j)\exp(-2\pi\sqrt{-1}jk/n), \quad \hat{u}_k^n(0) = \sum_{j=0}^{n-1} u_0(y_j)\exp(-2\pi\sqrt{-1}jk/n).$$

Concerning the differential equations, we have an issue: functions of the form (39) cannot, in general, satisfy the first two equations in (37) due to the nonlinear terms. This is because

$$F^n(y,t) = -\alpha_L p(v^n)(y,t) + \alpha_L^2\left(\frac{u_y^n}{v^n}\right)(y,t) \tag{40}$$

contains modes of wave number k outside $\{-n/2, -n/2+1, \dots, n/2-1\}$. However,

$$F_{\mathrm{ps}}^n(y,t) = \frac{1}{n}\sum_{k=-n/2}^{n/2-1}(-1)^k \hat{F}_k^n(t)\exp(\sqrt{-1}ky)$$

with

$$\hat{F}_k^n(t) = \sum_{j=0}^{n-1} F^n(y_j,t)\exp(-2\pi\sqrt{-1}jk/n)$$

[6] After computing $\{\hat{v}_k^n(t), \hat{u}_k^n(t)\}$, we set $\hat{v}_{-n/2}^n(t) = \hat{u}_{-n/2}^n(t) = 0$ to ensure that $v^n(y,t)$ and $u^n(y,t)$ given by (39) are real numbers. We also do the same thing for $\hat{F}_k^n(t)$ appearing below. The effect of such alternation is small when n is large.

gives an approximation of $F^n(y,t)$ when n is large enough (the approximation is exact at $y = y_j$); here, we can calculate $F^n(y_j,t)$ from $\{\hat{v}_k^n(t), \hat{u}_k^n(t)\}$ using (39) and (40). It is then natural to define the time evolution of $\{\hat{v}_k^n(t), \hat{u}_k^n(t)\}$ by

$$\begin{cases} \dfrac{d\hat{v}_k^n}{dt} = \sqrt{-1}\alpha_L k \hat{u}_k^n, & t > 0, \\ \dfrac{d\hat{u}_k^n}{dt} = \sqrt{-1} k \hat{F}_k^n, & t > 0. \end{cases}$$

This system is then numerically solved using the classical fourth-order Runge–Kutta method (we denote by Δt the time step).

From the computational point of view, it is important to note that $\hat{F}_k^n(t)$ can be computed effectively from $\{\hat{v}_k^n(t), \hat{u}_k^n(t)\}$ using fast Fourier transforms. Moreover, since the Fourier coefficients of a smooth function decay rapidly, this scheme is especially efficient when the solution to (19) is smooth (see [1] for a more detailed account); this is the case when the initial data are smooth.

4.2. **Long-time behavior of the fluid velocity at the origin.** We now numerically investigate the long-time behavior of $U(t) := u(0,t)$ for the solution (v,u) to (19). We set $t_i = i\Delta t$ and

$$U_i := u_{n/2}^n(t_i) = u^n(0,t_i) \quad (i = 0, 1, \dots, M := \lfloor T/\Delta t \rfloor),$$

where $\{u_j^n(t_i)\}$ are computed using the scheme explained in the previous section. We consider two initial data, one satisfying (i) $M_1^2 \neq M_2^2$ and the other (ii) $M_1^2 = M_2^2$, corresponding to Corollaries 2.3 and 2.4, respectively. Here, M_i is defined by (20). Note that we have

$$M_2 + M_1 = \frac{p''(1)}{2c^2} \int_{-\infty}^{\infty} u_0(x)\,dx, \quad M_2 - M_1 = \frac{p''(1)}{2c} \int_{-\infty}^{\infty} (v_0 - 1)(x)\,dx. \tag{41}$$

We suppose that $U(t)$ obeys a power-law of the form

$$U(t) = c_1 t^{-\alpha_1} + O(t^{-\alpha_2}) \quad (t \to \infty) \tag{42}$$

for some $0 < \alpha_1 < \alpha_2$ and $c_1 \neq 0$. We then numerically evaluate the exponent α_1 by the methods described in Appendix A. The first method is to apply (least squares) linear regression to the data

$$\{(\log_{10} t_i, \log_{10} |U_i|)\}_{i=M'}^{M}, \tag{43}$$

where $M' = \lfloor 0.95M \rfloor$.[7] If the obtained linear fit is $\log_{10}|U_i| \approx -\hat{\alpha}_1 \log_{10} t_i + c$ ($\hat{\alpha}_1, c \in \mathbb{R}$), then the slope $\hat{\alpha}_1$ is an estimator of α_1; the second method is to compute

$$Y_i = \frac{U_i - U_{i/2}}{U_{i/2} - U_{i/4}} \quad (i \equiv 0 \mod 4).$$

Then $y_i = -\log_2 Y_i$ is expected to converge to α_1 as $i \to \infty$. These approaches, however, require the maximum computation time T to be rather large. Therefore, we also consider accelerated versions: for the linear regression method, instead of the data (43), we use Richardson extrapolation, that is, we apply linear regression to the data

$$\{(\log_{10} t_i, \log_{10} |U_i^{(\gamma)}|)\}_{i=M'}^{M}$$

[7] More precisely, we use a subset of this data set: $\{(\log_{10} t_i, \log_{10}|U_i|) \mid M' \le i \le M,\ i \equiv 0 \mod P\}$ with $P = \lfloor M/160 \rfloor$. The effect of such omission is usually very small.

where γ is a positive number and

$$U_i^{(\gamma)} = U_i - 2^{-\gamma} U_{i/2} \quad (i \equiv 0 \mod 2). \tag{44}$$

With an appropriate choice of γ, the slope $\hat{\alpha}_1^{(\gamma)}$ of the linear fit $\log_{10} |U_i^{(\gamma)}| \approx -\hat{\alpha}_1^{(\gamma)} \log_{10} t_i + c^{(\gamma)}$ is expected to be a better estimator of α_1 than $\hat{\alpha}_1$; for the method using Y_i, we apply Aitken extrapolation, that is, we use

$$Z_i = Y_i - \frac{(Y_i - Y_{i/2})^2}{Y_i - 2Y_{i/2} + Y_{i/4}} \quad (i \equiv 0 \mod 16)$$

instead of Y_i. Then $z_i = -\log_2 Z_i$ is expected to converge to α_1 faster than y_i.

4.2.1. *Case (i): $M_1^2 \neq M_2^2$.* For an example of initial data satisfying $M_1^2 \neq M_2^2$, we consider

$$(v_0 - 1)(x) = u_0(x) = \frac{\exp(-x^2)}{\sqrt{\pi}}.$$

In this case, by (41), we have

$$M_2^2 - M_1^2 = (M_2 + M_1)(M_2 - M_1) \neq 0.^{8}$$

We set the parameters of the numerical simulation as follows:

$$(N, L, \Delta t, T) = (2^{14}, 3200, 10^{-3}, 1600).$$

In particular, $M = 1600000$.

From the obtained data of $\{U_i = u^n_{n/2}(t_i)\}_{i=0}^M$, we estimated the exponent α_1 of the power-law (42); see Figure 3. The obtained estimators of α_1 are

$$\hat{\alpha}_1 = 1.4972179393, \quad \hat{\alpha}_1^{(2)} = 1.5007380639$$

and

$$y_M = 1.4937167307, \quad z_M = 1.4988693297.$$

The choice $\gamma = 2$ in (44) is based on the method described in Appendix A (see the third paragraph of Section A.1). These support the theoretical result $\alpha_1 = 3/2$ (Corollary 2.3).[9]

To assess the accuracy of the results above, we vary the parameters $(N, L, \Delta t, T)$ and compare the results obtained with the ones above. Let us denote the reference parameters by

$$(N_0, L_0, \Delta t_0, T_0) = (2^{14}, 3200, 10^{-3}, 1600),$$

and we consider parameters of the form

$$(N, L, \Delta t, T) = (rN_0, rL_0, s\Delta t_0, T_0/s).$$

In Table 1, we list $(\hat{\alpha}_1, \hat{\alpha}_1^{(2)}, y_M, z_M)$ for three values of (r, s). We see that the effect of the variations of the parameters are small.

[8] More precisely, we have $(M_1, M_2) = (0, 1)$ and hence $M_2^2 - M_1^2 = 1$. By Corollary 2.3, this implies that the final sign of $u(0, t)$ is negative, and our numerical results are consistent with this prediction.

[9] We note that Case (i) is somewhat special in the sense that $M_1 = 0$. To avoid this particularity, we also analyzed initial data with $(M_1, M_2) = (2, 1)$ and still obtained results consistent with $\alpha_1 = 3/2$.

4.2.2. *Case (ii):* $M_1^2 = M_2^2$. For an example of initial data satisfying $M_1^2 = M_2^2$, we consider

$$(v_0 - 1)(x) = 0, \quad u_0(x) = \frac{\exp(-x^2)}{\sqrt{\pi}}.$$

In this case, by (41), we have

$$M_2^2 - M_1^2 = (M_2 + M_1)(M_2 - M_1) = 0.$$

We set the parameters of the numerical simulation as follows:

$$(N, L, \Delta t, T) = (2^{16}, 12800, 10^{-3}, 6400).$$

In particular, $M = 6400000$.

From the obtained data of $\{U_i = u^n_{n/2}(t_i)\}_{i=0}^M$, we estimated the exponent α_1 of the power-law (42); see Figure 4. The obtained estimators of α_1 are

$$\hat{\alpha}_1 = 1.7471572472, \quad \hat{\alpha}_1^{(3)} = 1.7501405988$$

and

$$y_M = 1.7378867212, \quad z_M = 1.7530938949.$$

The choice $\gamma = 3$ in (44) is based on the method described in Appendix A. By Corollary 2.4, we conjecture that $\alpha_1 = 7/4$; the results above support this conjecture.

To assess the accuracy of the results above, we vary the parameters $(N, L, \Delta t, T)$ and compare the obtained results with the ones above. Let us denote the reference parameters by

$$(N_0, L_0, \Delta t_0, T_0) = (2^{16}, 12800, 10^{-3}, 6400),$$

and we consider parameters of the form

$$(N, L, \Delta t, T) = (rN_0, rL_0, s\Delta t_0, T_0/s).$$

In Table 2, we list $(\hat{\alpha}_1, \hat{\alpha}_1^{(3)}, y_M, z_M)$ for three values of (r, s). We see that the effect of the variations of the parameters are small.

TABLE 1. Estimated values of the power-law exponent with different parameters for Case (i).

(r, s)	$\hat{\alpha}_1$	$\hat{\alpha}_1^{(2)}$	y_M	z_M
$(1.0, 1.0)$	1.4972179393	1.5007380639	1.4937167307	1.4988693297
$(0.5, 2.0)$	1.4972179582	1.5007381195	1.4937167305	1.4988693286
$(0.375, 2.5)$	1.4972179512	1.5007381002	1.4937167305	1.4988693286

Acknowledgements. This work was supported by Grant-in-Aid for JSPS Research Fellow (Grant Number 20J00882).

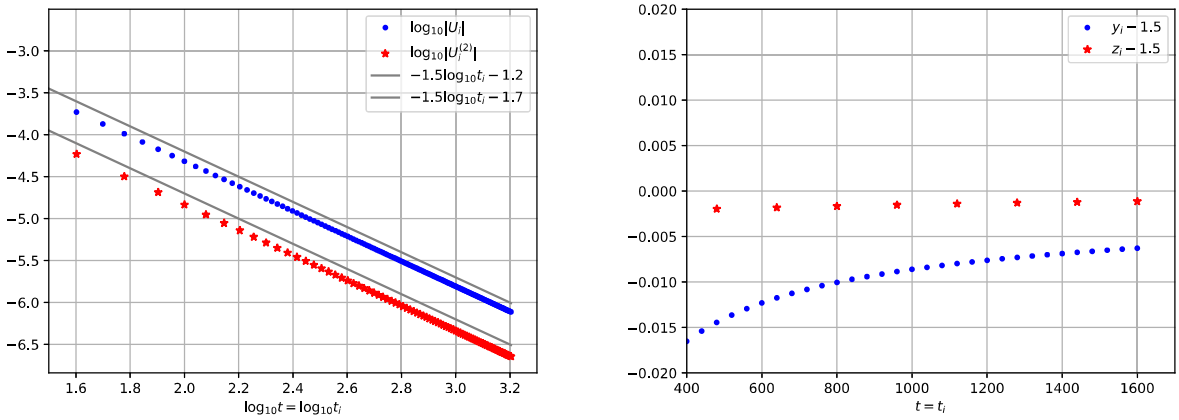

FIGURE 3. Left: The dotted markers represent $(\log_{10} t_i, \log_{10} |U_i|)$ and the star-shaped markers represent $(\log_{10} t_i, \log_{10} |U_i^{(2)}|)$ for Case (i); two lines have slope -1.5 and are displayed for comparison. Right: The dotted markers represent $(t_i, y_i - 1.5)$ and the star-shaped markers represent $(t_i, z_i - 1.5)$ for Case (i).

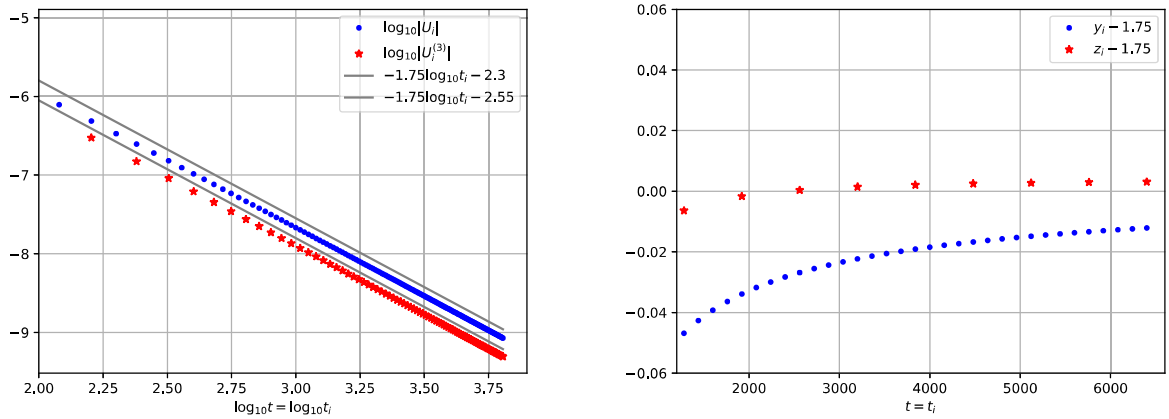

FIGURE 4. Left: The dotted markers represent $(\log_{10} t_i, \log_{10} |U_i|)$ and the star-shaped markers represent $(\log_{10} t_i, \log_{10} |U_i^{(3)}|)$ for Case (ii); two lines have slope -1.75 and are displayed for comparison. Right: The dotted markers represent $(t_i, y_i - 1.75)$ and the star-shaped markers represent $(t_i, z_i - 1.75)$ for Case (ii).

TABLE 2. Estimated values of the power-law exponent with different parameters for Case (ii).

(r, s)	$\hat{\alpha}_1$	$\hat{\alpha}_1^{(3)}$	y_M	z_M
$(1.0, 1.0)$	1.7471572472	1.7501405988	1.7378867212	1.7530938949
$(0.5, 2.0)$	1.7471500891	1.7501302295	1.7378870349	1.7530960383
$(0.375, 2.5)$	1.7471533349	1.7501347961	1.7378871839	1.7530968847

Appendix A. Power-law exponent estimation methods with sequence acceleration

Suppose that we are given a function $f = f(t)$ satisfying

$$f(t) = c_1 t^{-\alpha_1} + c_2 t^{-\alpha_2} + O(t^{-\alpha_3}) \quad (t \to \infty) \tag{45}$$

with $0 < \alpha_1 < \alpha_2 < \alpha_3$ and $c_1, c_2 \neq 0$. We present here some methods to evaluate the exponent α_1 from numerical data of $f(t)$. We also demonstrate theoretically and empirically that sequence acceleration methods are useful for such purpose; the idea is simple and the tools used are classical, but we could not find these methods in the literature. Therefore, we thought it would be beneficial to present these methods in an appendix, given the ubiquity of this task in science.

A.1. **Linear regression method; acceleration by Richardson extrapolation.** One simple way to evaluate α_1 in (45) is to apply (least squares) linear regression to the data

$$\{(\log_{10} t_i, \log_{10} |f(t_i)|)\}_{i=1}^{M},$$

where $0 < T' = t_1 < t_2 < \cdots < t_M = T$ and $t_{i+1} - t_i = \Delta t$. If

$$\log_{10} |f(t_i)| \approx -\hat{\alpha}_1 \log_{10} t_i + c$$

is the obtained linear fit, since

$$\log_{10} |f(t)| = -\alpha_1 \log_{10} t + \log_{10} |c_1| + O(t^{-(\alpha_2 - \alpha_1)}), \tag{46}$$

the slope $\hat{\alpha}_1$ gives us an approximation of α_1. We call this *the linear regression method*.

This approach, however, might require T' and T to be rather large when α_1 and α_2 are close; this is because the error term $O(t^{-(\alpha_2-\alpha_1)})$ in (46) may not decay fast enough. But if we have a guess of the exponent α_2 in (45), say, $\hat{\alpha}_2$, we can partially overcome this problem using Richardson extrapolation, that is, we apply linear regression to the data

$$\{(\log_{10} t_i, \log_{10} |f^{(\hat{\alpha}_2)}(t_i)|)\}_{i=1}^{M},$$

where

$$f^{(\hat{\alpha}_2)}(t) = f(t) - 2^{-\hat{\alpha}_2} f(t/2).$$

Since

$$f^{(\hat{\alpha}_2)}(t) = c_1(1 - 2^{\alpha_1 - \hat{\alpha}_2}) t^{-\alpha_1} + c_2(1 - 2^{\alpha_2 - \hat{\alpha}_2}) t^{-\alpha_2} + O(t^{-\alpha_3}),$$

if $|\alpha_2 - \hat{\alpha}_2|$ is small, the coefficient of $t^{-\alpha_2}$ becomes small; in particular, when $\alpha_2 = \hat{\alpha}_2$, we have

$$\log_{10} |f^{(\hat{\alpha}_2)}(t)| = -\alpha_1 \log_{10} t + \log_{10} |c_1(1 - 2^{\alpha_1 - \hat{\alpha}_2})| + O(t^{-(\alpha_3 - \alpha_1)}).$$

Then, since $\alpha_3 - \alpha_1 > \alpha_2 - \alpha_1$, we expect that the slope $\alpha_1^{(\hat{\alpha}_2)}$ of the linear fit

$$\log_{10} |f^{(\hat{\alpha}_2)}(t_i)| \approx -\hat{\alpha}_1^{(\hat{\alpha}_2)} \log_{10} t_i + c^{(\hat{\alpha}_2)}$$

gives a better approximation of α_1 than $\hat{\alpha}_1$. We also note that unless $\alpha_1 = \hat{\alpha}_2$, the leading order power-law exponent remains unchanged by altering $f(t)$ to $f^{(\hat{\alpha}_2)}(t)$.

One problem with this method is that we don't necessarily have a good guess of α_2. However, it is usually easier to have a guess of α_1, say, $\hat{\alpha}_1$. With such a guess, let us set

$$f^{(\hat{\alpha}_1)}(t) = f(t) - 2^{-\hat{\alpha}_1} f(t/2).$$

Then if $|\alpha_1 - \hat{\alpha}_1|$ is small, the coefficient of $t^{-\alpha_1}$ in

$$f^{(\hat{\alpha}_1)}(t) = c_1(1 - 2^{\alpha_1 - \hat{\alpha}_1})t^{-\alpha_1} + c_2(1 - 2^{\alpha_2 - \hat{\alpha}_1})t^{-\alpha_2} + O(t^{-\alpha_3})$$

is small; in particular, when $\alpha_1 = \hat{\alpha}_1$, we have

$$\log_{10} |f^{(\hat{\alpha}_1)}(t)| = -\alpha_2 \log_{10} t + \log_{10} |c_2(1 - 2^{\alpha_2 - \hat{\alpha}_1})| + O(t^{-(\alpha_3 - \alpha_2)}).$$

Therefore, the slope $\alpha_2^{(\hat{\alpha}_1)}$ of the linear fit

$$\log_{10} |f^{(\hat{\alpha}_1)}(t_i)| \approx -\hat{\alpha}_2^{(\hat{\alpha}_1)} \log_{10} t_i + c^{(\hat{\alpha}_1)}$$

is an estimator of α_2. In this way, we can numerically obtain a guess of α_2; in fact, the guesses $\hat{\alpha}_2 = 2$ and $\hat{\alpha}_2 = 3$ in Section 4 are obtained in this way.

Here, a remark may be of help to avoid unnecessary confusion: the guess $\hat{\alpha}_2$ obtained with the method above may return a value which is rather close to a higher order exponent. To understand this phenomenon, let us consider $f(t) = t^{-1/2} + 0.01t^{-1} + 10t^{-3/2}$. If we apply the method explained above with $T' = 950, T = 1000$, and $\Delta t = 6.25$, we obtain $\hat{\alpha}_2 = 1.4965435084$; this is because the coefficient 0.01 of t^{-1} is very small compared to 10 of $t^{-3/2}$. Thus, $\hat{\alpha}_2$ obtained in this way is an effective α_2 for the given data, which is closer to $-3/2$ than to -1.

If the technique above does not work well, we could also try Aitken extrapolation, which we shall explain in the next section.

A.2. **Ratio method; acceleration by Aitken extrapolation.** From the function $f = f(t)$, define a new function $Y = Y(t)$ by

$$Y(t) = \frac{f(t) - f(t/2)}{f(t/2) - f(t/4)}.$$

Then $-\log_2 Y(T)$ with T large gives an approximation of α_1 since

$$Y(t) = 2^{-\alpha_1} + 2^{-\alpha_1}(1 - 2^{\alpha_2 - \alpha_1})\frac{c_2(1 - 2^{\alpha_2})}{c_1(1 - 2^{\alpha_1})}t^{-(\alpha_2 - \alpha_1)} + O(t^{-\min\{2(\alpha_2 - \alpha_1), \alpha_3 - \alpha_1\}}).$$

We call this *the ratio method*.

Similar to the linear regression method, we need to take T large when α_1 and α_2 are close. This time, we can use Aitken extrapolation (Aitken Δ^2-process), that is, we define a new function $Z = Z(t)$ by

$$Z(t) = Y(t) - \frac{(Y(t) - Y(t/2))^2}{Y(t) - 2Y(t/2) + Y(t/4)}.$$

Then, by some calculations, we see that

$$Z(t) = 2^{-\alpha_1} + O(t^{-\min\{2(\alpha_2 - \alpha_1), \alpha_3 - \alpha_1\}}).$$

Hence, we expect that $-\log_2 Z(T)$ gives a better approximation of α_1 than $-\log_2 Y(T)$.

A.3. **An example.** Here, to empirically test the methods presented above, we consider the integral

$$f(t) = 2^{-1} \int_{t^{1/2}}^{t} (s + 1)^{-3/2}\, ds.$$

By an explicit computation, we see that

$$f(t) = (t^{1/2}+1)^{-1/2} - (t+1)^{-1/2} = t^{-1/4} - t^{-1/2} + O(t^{-3/4}). \tag{47}$$

Hence, we have $\alpha_1 = 1/4$, $\alpha_2 = 1/2$, and $\alpha_3 = 3/4$. Since $\alpha_2 - \alpha_1 = 1/4$ is quite small, as we shall see below, the methods without extrapolation give very bad estimates of α_1.

First, we apply the linear regression method with $T' = 9500, T = 10000$, and $\Delta t = 6.25$. We then obtain

$$\hat{\alpha}_1 = 0.21908886128, \quad \hat{\alpha}_1^{(1/2)} = 0.25282388874.$$

See Figure 5 (left). Note that the choice $\hat{\alpha}_2 = 1/2$ comes from (47). We clearly see that the method with Richardson extrapolation gives a much better estimate of $\alpha_1 = 1/4$. In fact, the linear regression method without extrapolation converges very slowly. For example, for $T' = 95000, T = 100000$, and $\Delta t = 6.25$, we get

$$\hat{\alpha}_1 = 0.23413598748, \quad \hat{\alpha}_1^{(1/2)} = 0.25081119797,$$

and $\hat{\alpha}_1$ is still quite far from $\alpha_1 = 1/4$.

Secondly, for the ratio method, we obtain

$$-\log_2 Y(10000) = 0.15519485047, \quad -\log_2 Z(10000) = 0.21677096182.$$

We see that $Y(10000)$ gives a very misleading value although $Z(10000)$ is also quite inaccurate. If we take $T = 100000$, we have

$$-\log_2 Y(100000) = 0.20693534152, \quad -\log_2 Z(100000) = 0.23976571677.$$

We can see that $-\log_2 Z(t)$ approaches to $\alpha_1 = 1/4$ much faster than $-\log_2 Y(t)$; see Figure 5 (right).

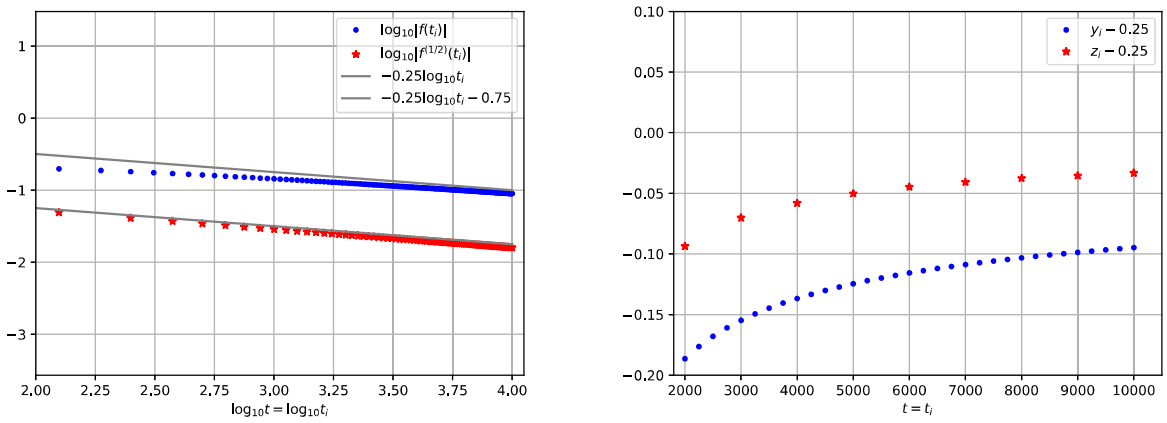

FIGURE 5. Left: The dotted markers represent $(\log_{10} t_i, \log_{10} |f(t_i)|)$ and the star-shaped markers represent $(\log_{10} t_i, \log_{10} |f^{(1/2)}(t_i)|)$; two lines have slope -0.25 and are displayed for comparison. We can observe that $(\log_{10} t_i, \log_{10} |f^{(1/2)}(t_i)|)$ deviates less from the reference line than $(\log_{10} t_i, \log_{10} |f(t_i)|)$. Right: In this graph, we write $y_i = -\log_2 Y(t_i)$ and $z_i = -\log_2 Z(t_i)$. The dotted markers represent $(t_i, y_i - 0.25)$ and the star-shaped markers represent $(t_i, z_i - 0.25)$. We can observe that $z_i - 0.25$ approaches to zero faster than $y_i - 0.25$.

REFERENCES

1. C. Canuto, M. Y. Hussaini, A. Quarteroni, and Zang T. A., *Spectral Methods in Fluid Dynamics*, Springer-Verlag, Heidelberg, 1988.
2. L. Du and H. Wang, *Pointwise wave behavior of the Navier-Stokes equations in half space*, Discrete Contin. Dyn. Syst. **38** (2018), 1349–1363.
3. K. Koike, *Refined pointwise estimates for the solutions to the one-dimensional barotropic compressible Navier–Stokes equations: An application to the analysis of the long-time behavior of a moving point mass*, https://arxiv.org/abs/2010.06578v1 (2020).
4. ———, *Long-time behavior of a point mass in a one-dimensional viscous compressible fluid and pointwise estimates of solutions*, J. Differential Equations **271** (2021), 356–413.
5. T.-P. Liu and S.-H. Yu, *On boundary relation for some dissipative systems*, Bull. Inst. Math. Acad. Sin. (N.S.) **6** (2011), 245–267.
6. ———, *Dirichlet-Neumann kernel for hyperbolic-dissipative system in half-space*, Bull. Inst. Math. Acad. Sin. (N.S.) **7** (2012), 477–543.
7. T.-P. Liu and Y. Zeng, *Large time behavior of solutions for general quasilinear hyperbolic-parabolic systems of conservation laws*, Mem. Amer. Math. Soc. **125** (1997), no. 599.
8. ———, *On Green's function for hyperbolic-parabolic systems*, Acta Math. Sci. Ser. B (Engl. Ed.) **29** (2009), 1556–1572.
9. D. Maity, T. Takahashi, and M. Tucsnak, *Analysis of a system modelling the motion of a piston in a viscous gas*, J. Math. Fluid Mech. **19** (2017), 551–579.
10. J. L. Vázquez and E. Zuazua, *Large time behavior for a simplified 1D model of fluid–solid interaction*, Comm. Partial Differential Equations **28** (2003), 1705–1738.
11. Y. Zeng, L^1 *asymptotic behavior of compressible, isentropic, viscous 1-D flow*, Comm. Pure Appl. Math. **47** (1994), 1053–1082.

GRADUATE SCHOOL OF ENGINEERING, KYOTO UNIVERSITY, KYOTO 615-8540, JAPAN
Email address: koike.kai.42r@st.kyoto-u.ac.jp